Research Square

Preprints are preliminary reports that have not undergone peer review.
They should not be considered conclusive, used to inform clinical practice,
or referenced by the media as validated information.

Quantum-inspired whale optimization framework applied to the qubit mapping problem

Hui Li
Harbin University of Commerce
Yingsong Ji
jiyingsong@hrbcu.edu.cn
Harbin University of Commerce
Jie Shen
Changzhou Vocational Institute of Mechatronic Technology
Jiepeng Wang
Harbin University of Commerce

Research Article

Keywords: Qubit mapping, Whale optimization algorithm, Quantum compiler design, Quantum-inspired algorithms, Combinatorial optimization

Posted Date: November 27th, 2026

DOI: https://doi.org/10.21203/rs.3.rs-10602147/v1

License: This work is licensed under a Creative Commons Attribution 4.0 International License.
Read Full License

Additional Declarations: No competing interests reported.

RESEARCH

Quantum-inspired whale optimization framework applied to the qubit mapping problem

Hui Li[1,2], Yingsong Ji[1,*], Jie Shen[3] and Jiepeng Wang[1]

[1]School of Computer and Information Engineering, Harbin University of Commerce, Harbin, 150028,China

[2]Heilongjiang Provincial Key Laboratory of Electronic Commerce and Information Processing, Harbin, 150028,China

[3]School of Information Engineering, Changzhou Vocational Institute of Mechatronic Technology, Changzhou, 213164, China

*Corresponding Author: Yingsong Ji. Email: **jiyingsong@hrbcu.edu.cn**

Received: Day Month Year; Accepted: Day Month Year; Published: Day Month Year

ABSTRACT: Qubit mapping under hardware connectivity constraints is a core bottleneck in the physical compilation pipeline of near-term quantum computing, as restricted physical topologies require inserting auxiliary SWAP operations that inevitably degrade overall gate fidelity. To address this NP-hard combinatorial problem, this paper proposes a quantum-inspired whale optimization framework (QI-WOF) that models discrete mapping configurations as continuous probability amplitudes within a unified Hilbert space. Specifically, we design a triple cooperative search paradigm. Within this paradigm, directional convergence is achieved via a quantum interference encircling mechanism utilizing constructive and destructive phase interference. Meanwhile, exploration diversity is sustained through a stochastic search driven by state collapse to escape local extrema. Furthermore, a phase-driven spiral tracking mechanism is introduced for continuous local refinement, which is supported by a nonlinear adaptive factor and quantum-state differential mutation to ensure stable state evolution. Numerical simulations on benchmark circuits demonstrate that the proposed framework consistently suppresses SWAP and CNOT gate overheads. Specifically, the proposed QI-WOF reduces the number of SWAP gates by an average of 68.27% compared to the baseline IBM_QX method, outperforming the industrial compilers t|ket> and Qiskit by 37.26% and 48.51%, respectively. These results confirm that applying continuous state evolutions to discrete qubit routing offers a robust, scalable, and high-performance solution for quantum compiler design.

KEYWORDS: Qubit mapping; Whale optimization algorithm; Quantum compiler design; Quantum-inspired algorithms; Combinatorial optimization

1 Introduction

Quantum computing has fundamentally transformed the paradigm of information processing by leveraging quantum superposition and entanglement. Specifically, the basic computational unit—the qubit—can exist in a coherent superposition of $|0\rangle$ and $|1\rangle$, while entanglement enables non-local correlations that have no classical counterpart[1-4]. As a result, quantum algorithms exhibit the potential for exponential speedups in particular problem domains, as exemplified by the reduced query complexity achieved in Simon's problem[5,6]. Nevertheless, within the noisy intermediate-scale quantum (NISQ) regime, practical quantum hardware is still subject to critical limitations, including restricted qubit connectivity, suboptimal gate fidelities, and limited coherence times. These constraints introduce substantial challenges for subsequent compilation processes, particularly due to mismatches between logical circuit structures and physical hardware to pologies[7,8]. In response, hybrid quantum–classical frameworks have been proposed, where algorithms such as the Variational Quantum Eigensolver[9] and the Quantum Approximate Optimization Algorithm combine quantum resources with classical optimization

to improve performance, although their effectiveness remains dependent on auxiliary classical strategies for scalability and convergence[10].

At the compilation level, one of the most critical challenges lies in the mapping of logical circuits onto hardware-constrained quantum devices. In practical implementations, limited coupling between physical qubits requires that non-adjacent two-qubit gates—commonly realized as CNOT operations—be decomposed into sequences of SWAP gates to enable qubit routing[11,12] This transformation inevitably increases circuit depth and introduces additional noisy operations, thereby degrading overall computational fidelity. To mitigate these effects, recent research has focused on intelligent optimization techniques and hardware-aware mapping strategies[13]. For example, hybrid approaches combining particle swarm optimization with reinforcement learning have demonstrated reduced gate overhead, while heuristic routing algorithms and graph neural network-based methods have shown improvements in execution efficiency and mapping quality[14-16]. Although these approaches effectively exploit hardware topology information, they largely rely on classical encoding schemes, which limits their ability to capture complex non-linear spatial correlations and restricts the exploration efficiency of the solution space[17].

Among various optimization strategies, swarm intelligence algorithms have attracted increasing attention due to their strong global search capability[18]. The Whale Optimization Algorithm (WOA)[19], inspired by the spiral foraging behavior of humpback whales, has demonstrated promising performance in routing and path planning problems. Building upon this foundation, several enhanced variants have been introduced to improve convergence behavior and avoid local optima. For instance, adaptive mechanisms based on decay factors enable dynamic adjustment of the search range, while crossover-based enhancements improve population diversity and prevent stagnation[20,21]. These advancements highlight the flexibility and robustness of WOA in handling high-dimensional optimization problems. In the context of quantum circuit mapping, such characteristics are particularly valuable for overcoming the limitations of conventional discrete encodings, which struggle to represent qubit entanglement relationships effectively. Furthermore, quantized extensions of WOA demonstrate that qubit-based representations can encode high-dimensional solution spaces more efficiently, alleviating the curse of dimensionality inherent in classical representations.

Despite these advances, the intrinsic computational complexity of the mapping problem remains a major obstacle. Quantum circuit mapping is an NP-hard combinatorial optimization problem, where the size of the solution space grows exponentially with the number of qubits[22]. This complexity is further exacerbated by hardware constraints, as the mapping between logical and physical qubits must satisfy limited connectivity, often requiring additional SWAP operations that expand both the search space and optimization difficulty. Classical metaheuristic algorithms provide a practical means to approximate high-quality solutions without exhaustive enumeration and can adapt their search strategies according to the underlying coupling graph. However, such methods are still prone to premature convergence due to population diversity loss, and their reliance on discrete encoding limits their ability to capture quantum structural information[23]. To address these limitations, this paper proposes a quantum-inspired whale optimization framework (QI-WOF) that models discrete mapping configurations as continuous probability amplitudes within a unified Hilbert space.

The primary contributions of this study are summarized as follows:

1 We introduce a continuous complex-valued vector representation combined with a probabilistic sampling mechanism for the qubit mapping problem. This formulation projects discrete topological configurations into normalized complex probability amplitudes, enabling a unified encoding scheme that preserves spatial correlations and avoids traditional discrete boundaries.

2 We propose a triple cooperative search paradigm within the QI-WOF architecture. This includes a phase-driven interference encircling mechanism, a stochastic state collapse search, and an adaptive phase-rotation spiral tracking mechanism. These operators cooperatively balance coherent global exploration and local refinement in the state space.

3 We design a nonlinear adaptive regulation factor based on fitness feedback, alongside a quantum mutation and crossover mechanism. Experimental evaluations across various benchmark circuits and

comparisons with industrial compilers demonstrate that the proposed framework consistently reduces SWAP gate overhead and CNOT counts, offering a stable and scalable solution for physical compiler design.

The remainder of this paper is organized as follows. Section 2 introduces the fundamental concepts of quantum computing and formulates the quantum circuit mapping problem under hardware constraints. Section 3 presents the proposed QI-WOF framework, including quantum state representation, improved search mechanisms, nonlinear adaptive regulation, and differential evolution strategies. Section 4 describes the application of QI-WOF to qubit mapping optimization, detailing the fitness function design and implementation procedure. Section 5 reports comprehensive experimental results, including comparisons with classical optimization algorithms, benchmark circuit evaluations, and industrial compiler analysis. Finally, Section 6 concludes the paper and discusses potential future research directions.

2 Quantum Circuit

2.1 Qubit

Quantum computing is a novel computational paradigm that manipulates quantum bits (qubits) in accordance with the fundamental principles of quantum mechanics. One of its core features is quantum state superposition, which allows qubits to exist simultaneously in a linear combination of multiple classical states, thereby enabling inherent parallelism in computation. The state of a single qubit can be expressed as **Eq. (1)**.

$$|\psi\rangle = \alpha\,|0\rangle + \beta\,|1\rangle \tag{1}$$

where $|0\rangle$ and $|1\rangle$ denote the computational basis states, α and β complex probability amplitudes satisfying the normalization condition $|\alpha|^2+|\beta|^2=1$. Owing to the complex-valued nature of these amplitudes, quantum interference arises when multiple quantum states are superposed. Through appropriately designed sequences of quantum gate operations, the interference effects can be manipulated to amplify the probability amplitude of a target state. During measurement, the qubit collapses to $|0\rangle$ with probability $|\alpha|^2$ and to $|1\rangle$ with probability $|\beta|^2$. By adjusting the phase of the probability amplitudes, constructive or destructive interference can be deliberately engineered, thereby enhancing the measurement probability of the desired target state $|0\rangle$ or $|1\rangle$.

2.2 Quantum Circuit Mapping

A quantum gate is an operation applied to qubits to manipulate and transform their quantum states. For example, the Hadamard (H) gate (matrix representation shown in **Fig. 1a)** acts on a single qubit to create a superposition state. The R*z*(θ) gate (matrix representation shown in **Fig. 1b**) operates on a single qubit to apply a phase rotation of θ around the Z-axis. For two-qubit systems, common operations include the CNOT gate (matrix representation shown in **Fig. 1c**), which flips the target qubit when the control qubit is in the $|1\rangle$ state, and the SWAP gate, which exchanges the states of two qubits and can be decomposed into three CNOT gates (as shown in **Fig. 1d**). Multi-qubit gates such as the Toffoli (CCNOT) gate [24] and the three-qubit parity gate [25] are less frequently used but remain indispensable in specific scenarios.

$$\mathrm{H} = \frac{1}{\sqrt{2}}\begin{bmatrix}1 & 1\\ 1 & -1\end{bmatrix} \qquad R_z(\theta) = \begin{bmatrix}e^{-i\theta/2} & 0\\ 0 & e^{i\theta/2}\end{bmatrix} \qquad \mathrm{CNOT} = \begin{bmatrix}1&0&0&0\\0&1&0&0\\0&0&0&1\\0&0&1&0\end{bmatrix} \qquad \mathrm{SWAP} = \begin{bmatrix}1&0&0&0\\0&0&1&0\\0&1&0&0\\0&0&0&1\end{bmatrix}$$

(a) **(b)** **(c)** **(d)**

Figure 1:(a) The matrix representation of the H gate; (b) The matrix representation of $R_z(\theta)$; (c) The matrix representation of the CNOT gate; (d) The matrix representation of the SWAP gate.

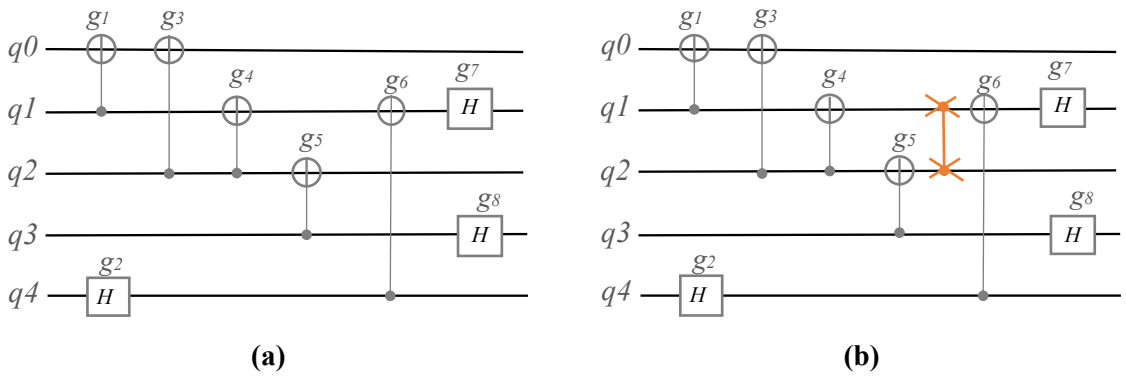

Figure 2: (a) Initial quantum circuit; (b) Quantum circuit satisfying physical constraints.

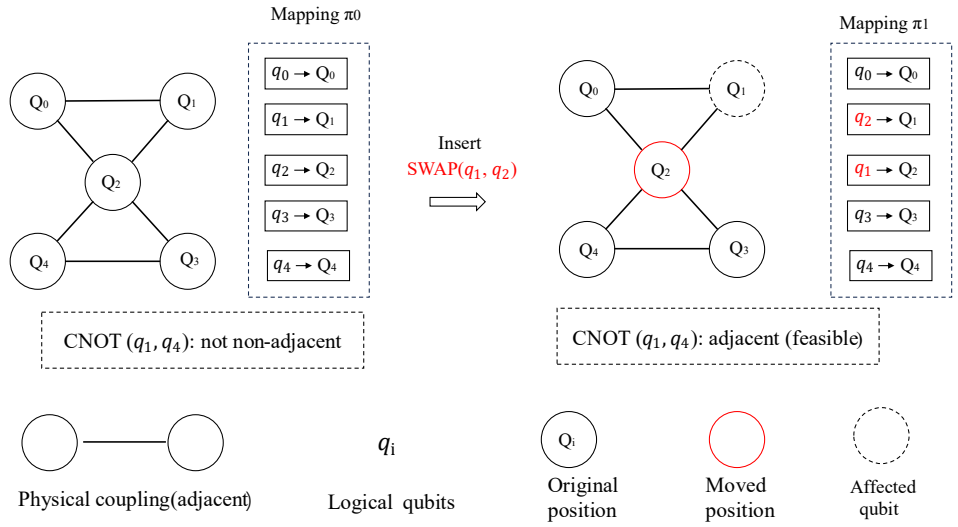

Figure 3: Evolution of logical-to-physical qubit mapping for executing CNOT(q1, q4) on the given coupling architecture.

Quantum Circuit Mapping is the process of converting abstract logical expressions into executable circuits that satisfy the topological constraints of specific physical devices . In current NISQ devices, the limited connections between physical qubits inside the quantum chip make SWAP gate operations necessary. In the hardware topology of IBM QX4[26], some physical qubits have direct coupling relationships due to their adjacent spatial positions.

A quantum circuit consists of multiple qubits and the sequences of quantum gates applied to them, where each horizontal line represents a logical qubit and quantum gates are arranged sequentially from left to right according to temporal order. **Fig. 2** illustrates the core challenges in quantum circuit mapping. In **Fig. 2a**, the circuit contains five logical qubits and eight quantum gates, with g_2, g_7 and g_8 being H gates and the remaining gates being CNOT gates. To map this circuit onto the IBM QX4 device, logical qubits must first be assigned to physical qubits. If a direct mapping scheme $q_i \rightarrow Q_i$ $(i = 0, \ldots, 4)$ is adopted, the qubit pair involved in gate g_6 (q_1, q_4) does not satisfy the coupling constraints of QX4 and cannot be executed directly. To meet connectivity requirements, SWAP gates must be inserted **(Fig. 2b)** to bring the relevant qubits adjacent to each other, ensuring that all quantum gates can be implemented. However, this increases the circuit depth, introduces additional noise, and reduces the overall fidelity of the algorithm. **Fig. 3** illustrates the circuit mapping evolution process.

Therefore, from the perspective of computational complexity, the quantum circuit mapping problem can be rigorously formulated as a combinatorial optimization problem. Given a logical quantum circuit Q, a hardware coupling graph $G = (V,E)$, and an integer k, the decision version aims to determine whether there exists a mapping strategy that satisfies the connectivity constraints of G while requiring no more than $k$inserted SWAP operations. In contrast, the optimization version seeks to minimize the value of k. The input elements of this problem include the logical qubit set $Q = \{q_1, \dots, q_n\}$and its corresponding sequence of quantum operations (primarily consisting of single-qubit gates and CNOT gates), as well as the coupling graph $G = (V,E)$, describing the physical device topology, where $V = \{v_1, \dots, v_p\}$denotes the set of physical qubits and Edefines the connectivity relationships that permit direct two-qubit interactions. The core objective of the solution process is to determine an injective mapping function $f: Q \to V$, which maps logical qubits onto physical qubits while satisfying hardware constraints and minimizing the number of inserted SWAP operations.

3 Algorithm Introduction

3.1 Whale Optimization Algorithm (WOA)

The Whale Optimization Algorithm (WOA), proposed by Mirjalili et al., is inspired by the foraging behavior of humpback whales, particularly their three characteristic strategies: prey encirclement, random search, and the spiral bubble-net feeding.

(1) Prey Encirclement

WOA simulates the encircling behavior of whales to guide individuals toward the current best solution.

(2) Random Search

When individuals deviate from the optimal solution, expanding the search range through random position perturbations enhances global search capabilities and maintains population diversity.

(3) Bubble-Net Feeding

By employing a spiral approximation strategy, individuals are guided along a curved trajectory toward the optimal solution, thereby enhancing local search accuracy and improving convergence stability.

3.2 Quantum-inspired Whale Optimization Framework (QI-WOF)

WOA relies on contraction-envelopment and spiral approximation to achieve global convergence; however, its linear decay and geometric contraction trajectories struggle to adapt to the highly irregular nature of the qubit mapping space, making it prone to repeated searches on complex coupling graphs. Furthermore, the real-number encoding used by WOA cannot express complex-valued phase relations and joint statistical dependencies between qubit mappings, making it difficult to accurately assess mapping feasibility and gate sequence cost. To overcome these limitations, QI-WOF introduces quantum state superposition, interference phase control, and differential evolution perturbation mechanisms to enhance search diversity and structural adaptability.

3.2.1 Quantum-Inspired State Representation of Individuals

Classical optimization algorithms often incur substantial computational overhead due to large population sizes and complex encoding schemes, and they may also exhibit limited efficiency in exploring high-dimensional solution spaces. To address these limitations, the QI-WOF algorithm encodes each individual using a quantum state vector representation, formulated as follows:

$$|\psi\rangle = \sum_{i=1}^{N} \alpha_i |i\rangle, \quad \sum_{i=1}^{N} |\alpha_i|^2 = 1 \tag{2}$$

where the complex amplitudes characterize the distribution of an individual over different candidate solutions and satisfy the normalization constraint.

During the population initialization phase, the algorithm generates multiple independent individuals by repeating the procedure according to the predefined population size P, formulated as follows:

$$\mathrm{P}(0) = \{\psi_1, \psi_2, \ldots, \psi_P\} \tag{3}$$

To ensure balanced exploration, the initial states are generated according to a uniform probability distribution, the mathematical formulation is shown in **Eq. (4)**,

$$\alpha_i = \frac{1}{\sqrt{N}}, \quad i = 1, 2, \ldots, N \tag{4}$$

Under this condition, all candidate solutions have equal initial probabilities, thereby avoiding bias in the early stages of the search. Subsequently, the initial candidate solution set is obtained through a probabilistic sampling mechanism, serving as the input for subsequent evolutionary iterations.

3.2.2 Improved Search Strategy

In the classical WOA, although update strategies such as "encircling prey" and "spiral tracking" can to some extent balance global exploration and local exploitation, they fundamentally rely on linear or geometric convergence trajectories. This reliance limits their adaptability to the multimodal characteristics of high-dimensional, complex optimization problems, resulting in insufficient search diversity, rigid convergence paths, and a tendency to become trapped in local optima. To address these issues.

(1) Quantum Interference Encircling Mechanism (QIEM):

Quantum interference arises from the linear superposition and phase correlation of quantum states. Let two normalized quantum states be $|\psi_1\rangle$and $|\psi_2\rangle$, whose superposition forms a new state $|\psi\rangle$, formulated as follows:

$$|\Psi\rangle = \alpha |\psi_1\rangle + \beta e^{i\theta} |\psi_2\rangle \tag{5}$$

After normalization, the squared amplitude determines the measurement probability distribution. By modeling state representations using complex numbers, the proposed algorithm mathematically simulates constructive or destructive interference effects, which can amplify or suppress specific candidate solutions based on the phase difference θ. In the algorithm design, this mechanism enables the classical optimization framework to concurrently evaluate multiple potential path trajectories and amplify the probabilities of favorable ones through interference. In contrast, although the classical WOA can guide individuals toward $\bar{X}_{best}$ via the "encircling prey" mechanism, its linear convergence often results in insufficient local exploitation in complex multimodal spaces. To overcome this limitation, QI-WOF draws on WOA's contraction-update concept and replaces the linear contraction with quantum interference operations, thereby proposing a QIEM. Specifically, by superposing the complex probability amplitudes of the current state $|\psi_i(t)\rangle$ and the optimal state $|\psi^*(t)\rangle$, directional search trajectories are formed in the probability space, thereby effectively enhancing search diversity and robustness while maintaining the convergence trend, formulated as follows:

$$|\psi_i(t+1)\rangle = \mathrm{Norm}\left(|\psi_i(t)\rangle + e^{i\theta} \cdot |\psi^*(t)\rangle\right), \quad \theta \sim U(0, 2\pi) \tag{6}$$

Here, "Norm"(·) denotes the normalization operation for complex numbers.

(2) Quantum Random Search Mechanism (QRSM):

The probabilistic sampling of the simulated quantum states is inherently stochastic, naturally generating diverse candidate solutions in the probability space. Inspired by the "global exploration based on $\bar{X}$

concept in WOA, QI-WOF introduces a QRSM, wherein a randomly selected whale state $|\psi_r\rangle$interferes with $|\psi_i\rangle$, the mathematical formulation is shown in **Eq. (7)**:

$$|\psi_i(t+1)\rangle = \mathrm{Norm}\left(|\psi_i(t)\rangle + e^{i\theta}\cdot|\psi_r(t)\rangle\right), \quad \theta \sim U(0,2\pi) \tag{7}$$

Subsequently, during the measurement phase, collapse sampling is performed according to the probability distribution to achieve nonlinear jumps. This mechanism preserves the stochasticity inherent in the exploration process while avoiding the blind search characteristic of conventional WOA, thereby expanding the search coverage while maintaining a bias toward potentially high-quality solutions.

(3) Quantum Spiral Tracking Mechanism (QSTM):

The WOA employs a logarithmic spiral function to iteratively approach $\overrightarrow{X_{best}}$, enhancing search precision. However, **Eq. (8)** demonstrates limited adaptability in high-dimensional complex problems, as it struggles to adjust step size and direction flexibly, often leading to local optima.

$$\vec{X}(t+1) = \overrightarrow{D'}\cdot e^{bl}\cdot\cos(2\pi l) + \overrightarrow{X_{best}}(t) \tag{8}$$

To address this, a QSTM is introduced, whose mathematical formulation is given in **Eq. (9)**: a phase rotation is applied to $|\psi_i(t)\rangle$ and interfered with $\psi^*(t)$ to emulate the mathematical characteristics of WOA's spiral convergence. Unlike conventional spirals based on geometric distance, the quantum spiral tracking generates a phase-driven, directionally convergent trajectory in probability space, enabling the new state $|\psi_i(t+1)\rangle$ to retain perturbation amplitude while approaching the optimum. This not only refines local search capability but also maintains diversity in the neighborhood of optimal solutions.

$$|\psi_i(t+1)\rangle = \mathrm{Norm}\left(e^{ibl}\cdot|\psi^*(t)\rangle + e^{i2\pi l}\cdot|\psi_i(t)\rangle\right), \quad l \sim U(-1,1) \tag{9}$$

Here, l is a perturbation parameter controlling the rotation amplitude, uniformly sampled from $[-1,1]$, and b is the spiral control constant, which regulates the rotation extent of the optimal state.

3.2.3 Nonlinear Adaptive Regulation Factor

In the classical WOA, **Eq. (10)** exhibits limitations in complex optimization problems[27]: first, overly rapid decay can cause the algorithm to lose exploration capability prematurely, leading to entrapment in local optima; second, overly slow decay may delay convergence toward high-precision solutions.

$$\vec{A} = 2\vec{a}\cdot\vec{r} - \vec{a} \tag{10}$$

To address these issues, this study introduces a nonlinear decay factor *a(t)*, which is adaptively adjusted in conjunction with the fitness improvement rate to achieve a dynamic balance between exploration and exploitation. The mathematical formulation is shown in **Eq. (11)**

$$a(t) = \mathrm{clip}\left[a_0\cdot\left(1-\left(\frac{t}{T}\right)^{\kappa}\right)\cdot\left(1+\sigma\cdot\frac{f_{t-\Delta}-f_t}{|f_{k-\Delta}|}\right), \quad a_{\min}, a_0 \right] \tag{11}$$

$$a_{base}(t) = a_0\left(1-\left(\frac{t}{T}\right)^{\kappa}\right) \tag{12}$$

$$a_{\text{adapt}}(t) = 1 + \sigma \cdot \frac{f_{t-\Delta} - f_t}{|f_{t-\Delta}|} \tag{13}$$

Here, $a_{base}(t)$ represents a decay factor, as defined in **Eq. (12)**, which progressively decreases the intensity of random search with increasing iterations. The parameter k is set to 1.6. Furthermore, $a_{adapt}(t)$ denotes an adaptive adjustment term, whose mathematical formulation is given in **Eq. (13)**. It dynamically regulates the convergence rate and adaptively balances exploration and exploitation according to the optimization process, thereby effectively avoiding entrapment in local optima. $f_{t-\Delta} - f_t$ denotes the fitness improvement over the past Δiterations, and $|f_{t-\Delta}|$ prevents division by zero while normalizing the improvement rate, with the adaptive coefficient σ set to 0.4.

3.2.4 Differential evolution

Differential Evolution (DE) [28] is a classical population-based intelligent optimization method. Its core principle is to generate mutant vectors through differential operators during individual updates and to produce new candidate solutions via crossover, thereby enhancing the global search capability and population diversity. Within the QI-WOF algorithmic framework, the **Eq. (14)** is employed to update the positions of whale individuals, where a mutation–crossover procedure is activated with a probability P_{DE} to generate new solutions. This mechanism strengthens population perturbation and mitigates premature convergence.

$$V_i = \psi_a + F \cdot (\psi_b - \psi_c) \tag{14}$$

Among them,ψ_a,ψ_b,and $\psi_c$are three randomly selected and mutually distinct quantum-state individuals. The parameter Fserves as the scaling factor that controls the magnitude of the differential term and is typically set to 0.7. The expression $(\psi_b - \psi_c)$denotes the directional difference between two quantum-inspired state vectors in the complex space, which is added to $\psi_a$to construct the mutant state individual V_i(Mutant Vector). This operation is equivalent to introducing a perturbation to the current solution along the direction defined by two randomly chosen individuals, thereby broadening the search trajectory and enhancing global exploratory jumps [30].

Subsequently, to maintain physical measurability, $V_i$undergoes a normalization process to ensure that it remains a valid quantum superposition state. The mutant vector $V_i$and the original individual ψ_i(Target Vector) are then combined through binomial crossover to form the trial state U_i(Trial Vector), formulated as follows:

$$U_i^{(j)} = \begin{cases} V_i^{(j)}, & \text{if } \text{rand}(j) \le CR \text{ or } j = j_{\text{rand}} \\ \psi_i^{(j)}, & \text{otherwise} \end{cases} \tag{15}$$

In this process, CR denotes the crossover rate, and j_{rand} ensures that at least one gene is inherited from the mutant vector. After the crossover operation is completed in the complex space, the resulting state is similarly subjected to a normalization procedure.

Fig. 4 illustrates the overall workflow of the proposed algorithm.

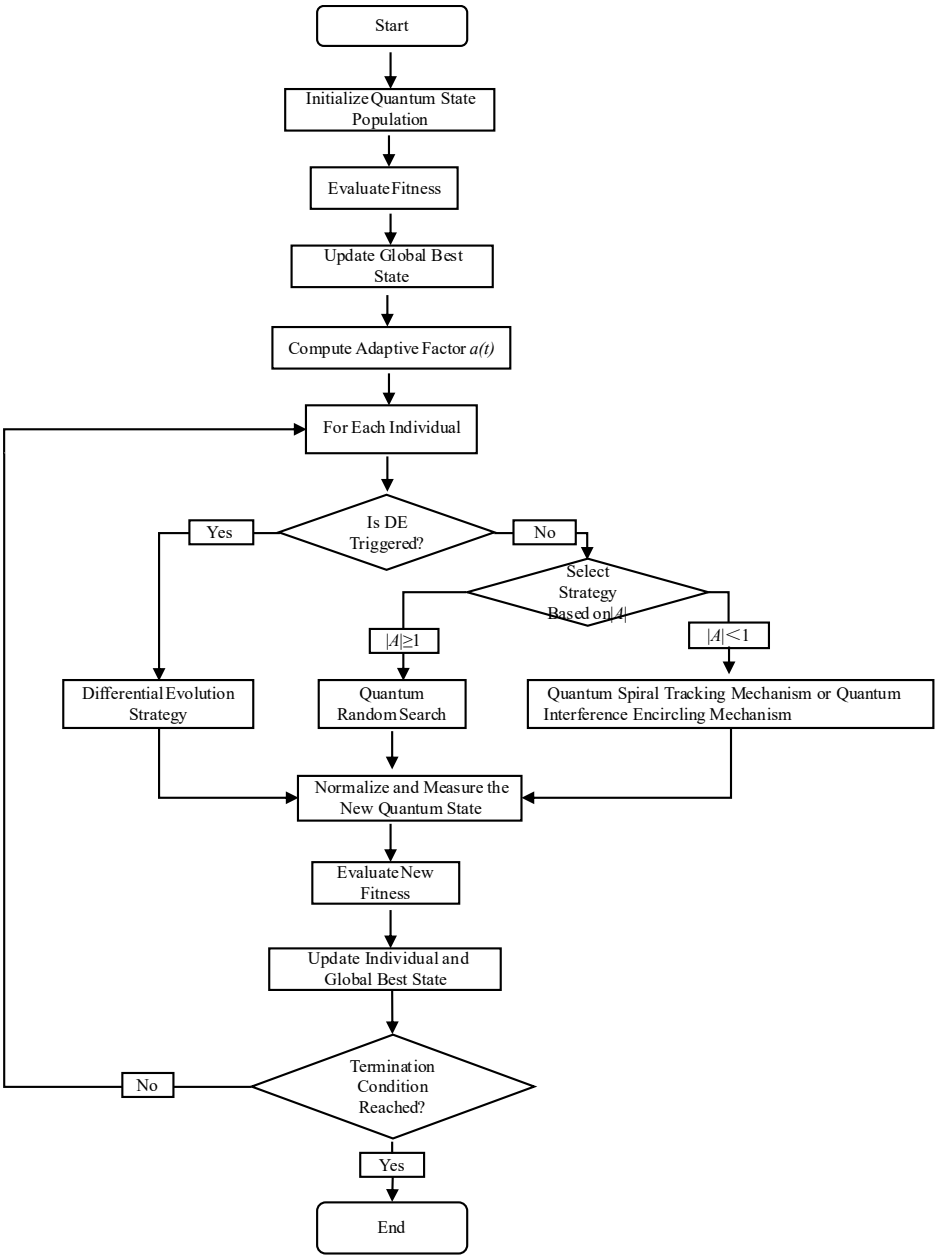

Figure 4: Procedure of the QI-WOF Algorithm.

4 Qubit Mapping Optimization Based on a Quantum-inspired Whale Optimization Framework

4.1 Algorithm Application

During the quantum circuit mapping process, individuals in QI-WOF are represented as quantum states, where each quantum state ψ_i encodes the probability distribution of a candidate mapping. The dimensionality of $\psi_i$equals the number of physical qubits N, and the squared amplitude $|\alpha_{ij}|^2$denotes the probability that logical qubit $i$is mapped to physical qubit j. In this manner, the algorithm is capable of concurrently representing and evolving a multi-state probability distribution across the mapping solution space. During population initialization, the algorithm generates a set of independent individuals according to the predefined population size, forming the initial population, after which quantum-state measurement is performed to obtain the initial candidate mapping structures.

During the search phase, **Eqs. (6)**, **(7)** and **(9)**. are introduced to achieve dynamic optimization of the mapping scheme. For instance, when executing the quantum interference encircling mechanism, if the optimal state ψ_t^* is superposed with the current state $|\psi_i(t)\rangle$, adjusting the phase difference θ is equivalent to searching for paths with low SWAP costs in the topology graph. Specifically, when $\theta = 0$, the superposition enhances the probability of candidate solutions similar to the optimal mapping; conversely, when $\theta = \pi$, it suppresses suboptimal solutions containing redundant CNOT operations.

Fig. 5 illustrates the quantum mapping process based on QI-WOF.

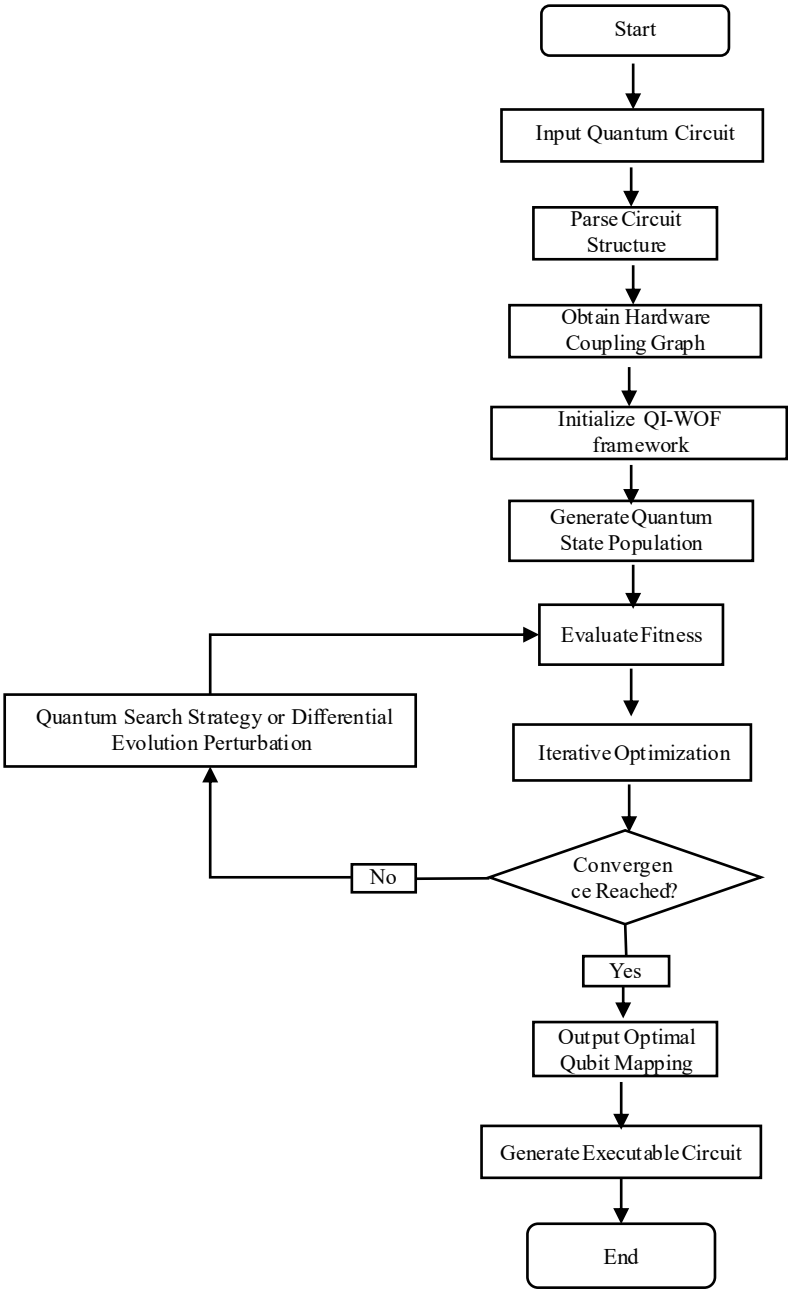

Figure 5: Qubit mapping workflow.

In the context of quantum circuit mapping, the proper construction of a fitness function is crucial to ensure that the optimization algorithm converges to high-quality solutions. Accordingly, this work designs

a fitness function tailored for QI-WOF during the quantum circuit mapping optimization process, formulated as follows:

$$f(x) = \omega_{SWAP} \cdot \mathrm{SwapCost}(x) + \omega_{CNOT} \cdot \mathrm{CNOTCost}(x) + \omega_{Depth} \cdot \mathrm{DepthCost}(x) \tag{16}$$

Since SWAP operations directly increase gate overhead and serial latency, they are highly sensitive to noise in NISQ devices. As the fundamental two-qubit gate, the number of CNOT gates is strongly correlated with the overall error rate. Although circuit depth affects parallelism, it can be partially mitigated through hardware topology optimization, formulated as follows:

$$\omega_{SWAP} > \omega_{CNOT} > \omega_{Depth} \tag{17}$$

In each iteration, candidate quantum-inspired state vectors collapse into concrete mapping schemes through measurement and are evaluated based on the comprehensive fitness function $f(x)$. If a new solution outperforms the current one, it is adopted and the global optimal state is updated. Otherwise, the crossover and mutation mechanisms of differential evolution are employed to maintain the exploratory capability of the population. As iterations progress, QI-WOF gradually converges to high-quality qubit mappings while preserving population diversity.

The specific steps for implementing the QI-WOF pan-optimized quantum circuit are as follows:

Step 1. QI-WOF first establishes physical topology constraints according to the coupling graph of the quantum chip, and initializes a population of quantum-inspired state vectors within the Hilbert space.

Step 2. Each quantum state encodes the probability distribution of candidate mapping solutions through complex amplitudes, which are normalized and probabilistically sampled to generate initial feasible solutions.

Step 3. During iteration, the algorithm adaptively adjusts the convergence step size via *a(t)*, while employing three quantum search mechanisms governed by parameter *A* to balance global exploration and local exploitation.

Step 4. Differential evolution operators are randomly triggered to perform mutation and crossover on selected quantum-inspired state vectors, introducing directional perturbations that enhance population diversity.

Step 5. The updated complex-valued state vectors are normalized and probabilistically sampled to generate concrete mapping solutions; their fitness is evaluated using *f(x)*, and superior solutions replace current individuals while updating the global optimum.

Step 6. Finally, QI-WOF outputs the globally optimal qubit mapping solution B_{best}, which determines the optimal execution path of the quantum circuit on the target hardware.

5 Experimental Results

To comprehensively evaluate the performance of the proposed QI-WOF algorithm, three groups of comparative experiments were designed and conducted.

First, within a unified framework of classical mathematical optimization problems, a variety of representative optimization algorithms were selected for horizontal comparison, enabling a comprehensive analysis of the advantages of QI-WOF in terms of robustness and convergence behavior.

Second, in the context of quantum circuit mapping, comparative experiments were performed on benchmark circuits of varying scales using the classical IBM_QX[29], WOA, and QI-WOF algorithms, with the aim of assessing the effectiveness of QI-WOF in practical problem settings.

Third, to evaluate its competitiveness in industrial applications, QI-WOF was compared with two mainstream commercial compilers. In addition, systematic comparisons were conducted with classical algorithms such as 2QAN[30], HQAA[31] and GA4QCO[32] under different compilation environments, which measure how the overhead varied across different benchmarks.

All experiments were carried out on a Windows 11 x64 operating system, equipped with an NVIDIA GeForce GTX 1650 Ti GPU and 11.7 GB of memory.

5.1 Algorithm Performance Evaluation

This section evaluates the performance of the proposed approach by employing five comparative algorithms, namely the Whale Optimization Algorithm (WOA), Grey Wolf Optimizer (GWO [33]), Particle Swarm Optimization (PSO [34]), Marine Predators Algorithm (MPA [35]), and Artificial Bee Colony (ABC [36]). The F10 function from the CEC2017[37] benchmark suite is selected as the test problem, as its complexity closely resembles that of the quantum circuit mapping problem. In order to comprehensively assess the performance of the proposed method, three key evaluation criteria are considered. First, convergence accuracy is quantified by recording the fitness value of the final solution obtained by each algorithm, where smaller values correspond to better optimization performance. Second, convergence speed is examined by analyzing the variation of fitness values throughout the iterative process, which reflects the efficiency of the search procedure. Third, robustness is evaluated through multiple independent runs, where each algorithm is executed 30 times to obtain statistical indicators, including the best, worst, mean, and standard deviation of the fitness values. The test parameter settings are shown in **Table 1**.

Table 2 presents the statistical results of the fitness values over 30 independent runs, highlighting the comparative stability and reliability of each algorithm. **Fig. 6** illustrates the convergence curves, depicting the evolutionary trajectories of fitness values during the optimization process. The results demonstrate that QI-WOF achieves faster objective value reduction in the initial phase, indicating enhanced global search capability. As the iterations progress, the integration of quantum-inspired encoding and differential evolution strategies helps sustain population diversity, enabling the algorithm to maintain steady convergence while avoiding premature stagnation. Consequently, QI-WOF not only reaches better fitness values with fewer iterations but also yields lower final errors, confirming its effectiveness and robustness in handling complex optimization tasks.

The mathematical formulation is given as follows:

$$f(x) = -20\exp\left(-0.2\sqrt{\frac{1}{d}\sum_{i=1}^{d}x_i^2}\right) - \exp\left(\frac{1}{d}\sum_{i=1}^{d}\cos(2\pi x_i)\right) + 20 + e \tag{18}$$

Table 1: Test parameter settings.

Population size	Maximum number of iterations	Number of runs	Parameters of the QI-WOF algorithm
30	50	30	DE-ratio=0.3、F=0.5、CR=0.7

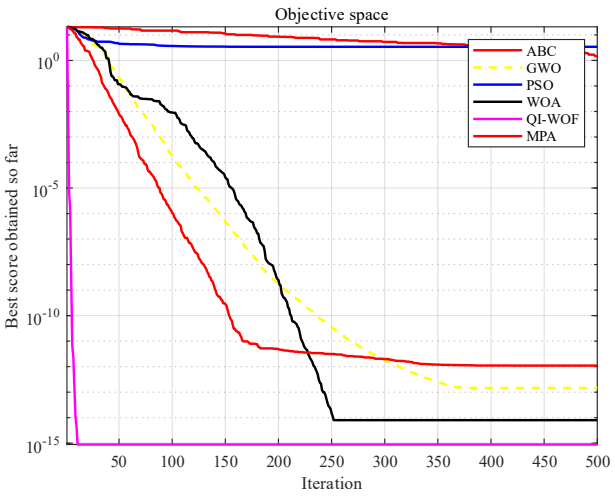

Figure 6: Comparison of algorithm accuracy.

Table 2: Comparison of Algorithm Fitness Function Values

Algorithm	Best	Worst	Mean	Std
WOA	8.88e-16	7.98e-15	5.17e-15	2.96e-15
GWO	7.57e-14	1.45e-13	1.03e-13	2.72e-14
PSO	3.44	6.03	4.75	1.05
MPA	6.85e-13	1.20e-13	9.29e-13	2.11e-13
ABC	1.32	2.32	1.56	0.42
QI-WOF	8.88e-16	8.88e-16	8.88e-16	0

5.2 Analysis of Optimization Results

To validate the effectiveness of the proposed algorithm in the quantum circuit mapping process, experiments were conducted on benchmark quantum circuits selected from the widely used B131 and B114 datasets. These benchmark sets encompass a variety of representative quantum circuits commonly employed in quantum compilation research. The number of qubits in these circuits ranges from 5 to 16, while the number of quantum gates varies approximately from 20 to 35,000. The primary evaluation metric is the number of inserted SWAP gates during the mapping process, which directly reflects the efficiency of the mapping strategy in handling limited qubit connectivity.

For comparison, the IBM_QX mapping algorithm was adopted as the baseline method. In addition, the Whale Optimization Algorithm (WOA), a classical swarm intelligence optimization approach, was included as a representative metaheuristic algorithm. By comparing QI-WOF with both a hardware-oriented heuristic method (IBM_QX) and a population-based optimization algorithm (WOA), the experimental design enables a comprehensive evaluation across different categories of mapping strategies.

Table 3 shows that QI-WOF consistently achieves lower SWAP gate counts across most benchmark circuits. Compared with the IBM_QX method, QI-WOF reduces the number of SWAP gates by an average of 68.27%, significantly decreasing the routing overhead. Compared with the classical WOA algorithm, QI-WOF further achieves an average improvement of 20.18%. In particular, for circuits such as qft_10, the improvement reaches 44.44%, demonstrating the effectiveness of the proposed hybrid strategy. The superior performance of QI-WOF over IBM_QX can be attributed to its global search capability enabled by quantum state representation and interference-driven exploration, which effectively overcomes the limitations of rule-based local heuristics. Compared with WOA, the proposed method enhances both exploration and exploitation through quantum interference mechanisms and differential evolution perturbations, thereby alleviating premature convergence and improving solution quality.

As a result, QI-WOF demonstrates stronger adaptability and scalability in handling complex quantum circuit mapping tasks, particularly for large-scale benchmark circuits.

Table 3: Experimental comparison of different qubit allocation algorithms.

Benchmark			SWAP count		
Name	qubit count	Input gate count	IBM_QX	WOA	QI-WOF
4mod5-v1_22	5	21	19	0	0
mod5mils_65	5	35	22	0	0
alu-v0_27	5	36	28	3	3
decod24-v2_43	4	52	19	0	0
4gt13_92	5	66	40	0	0
ising_model_10	10	480	22	0	0
ising_model_13	13	633	66	0	0
ising_model_16	16	786	114	0	0
qft_10	10	200	81	54	30
qft_13	13	403	184	86	80
qft_16	16	512	291	146	118
rd84_142	15	343	164	105	84
adr4_197	13	3439	1722	1614	912
radd_250	13	3213	1634	756	746
z4_268	11	3073	1449	712	634
misex1_241	15	4843	1927	182	132
cycle10_2_110	12	6050	2236	83	62
square_root_7	15	7630	2453	1438	1538
sqn_258	10	10223	4522	2130	2024
rd84_253	12	13658	5212	286	196
co14_215	15	17936	6864	524	365
sym9_193	11	34881	12574	8034	7682

5.3 Evaluation of Industrial Competitiveness

5.3.1 Comparative Analysis of Compiler Results

To further validate the practical industrial applicability of the proposed QI-WOF algorithm in real quantum computing environments, this section conducts a comparative analysis with mainstream industrial-grade quantum compilers. Specifically, two widely used quantum compilation platforms, t|ket>[38] and Qiskit[39], are selected as baseline benchmarks. By comparing the number of SWAP and CNOT operations during the optimization process, the mapping optimization capability of QI-WOF under different compilation environments is systematically evaluated. Furthermore, employing multiple compilers in the evaluation helps mitigate potential bias introduced by a single platform, thereby enabling a more comprehensive and reliable assessment of the industrial applicability and generalization capability of QI-WOF in quantum circuit mapping optimization.

Table 4 demonstrates that, compared with the native t|ket> compiler, the proposed QI-WOF algorithm significantly reduces the number of SWAP gates, achieving an average improvement of approximately 37.26%. This advantage becomes more pronounced for medium- and large-scale circuits ($\geqslant$12 qubits); for instance, at 12 qubits, the optimization rate reaches 43.67%. Meanwhile, the number of CNOT gates is

reduced by an average of 15.44%, with a maximum reduction of up to 22.81% observed in medium- and large-scale circuits. In comparison with the Qiskit compiler, QI-WOF achieves an average reduction of 48.51% in SWAP gate operations. For medium- and large-scale circuits, the reduction exceeds 50%, reaching as high as 69.11% at 22 qubits. In addition, the number of CNOT gates is reduced by an average of 14.10%, although slight fluctuations are observed in larger circuits.

These results confirm that QI-WOF provides consistent and scalable performance improvements.

Table 4 Comparison of gate counts across different compilers.

Compiler	Name	Original		QI-WOF		Improvement (%)	
	qubit count	SWAP count	CNOT count	SWAP count	CNOT count	SWAP count	CNOT count
t|ket>	4	8	15	6	13	25.00	13.33
	6	11	24	9	20	18.18	16.67
	8	18	30	12	26	33.33	13.33
	10	24	42	17	36	29.17	14.29
	12	35	45	18	41	48.57	8.89
	14	40	57	22	44	45.00	22.81
	16	43	64	24	55	46.51	14.06
	18	46	75	28	63	39.13	16.00
	20	58	82	33	71	43.10	13.41
	22	65	102	36	84	44.62	17.65
Qiskit	4	8	15	6	13	25.00	13.33
	6	10	24	9	20	10.00	16.67
	8	18	30	12	26	33.33	13.33
	10	28	43	17	38	39.29	11.63
	12	42	48	19	43	54.76	10.42
	14	55	57	21	45	61.82	21.05
	16	68	69	23	55	66.18	20.29
	18	75	78	30	76	60.00	2.56
	20	93	84	32	71	65.59	15.48
	22	123	105	38	88	69.11	16.19

5.3.2 Comparative Analysis of Results Across Different Algorithms

This experiment aims to systematically evaluate the optimization performance and stability of different algorithms in quantum circuit mapping, with a particular focus on how metric overhead evolves across various benchmarks when implemented on mainstream compilers (such as t|ket⟩ and Qiskit).

Specifically, this experiment uses the number of SWAP and CNOT operations as key evaluation metrics. The selected comparison algorithms—HQAA, 2QAN, and GA4QCO—represent a diverse range of optimization paradigms in quantum circuit mapping, including heuristic strategies, quantum heuristics, and evolutionary algorithms.

Fig. 7 and **Fig. 8** present the variation trends of SWAP and CNOT counts with increasing qubit numbers for all algorithms under t|ket⟩ and Qiskit. As the circuit scale grows, all methods show an overall increasing pattern in both metrics, with differences becoming more pronounced in the mid-to-large qubit range (approximately 12–22 qubits). Among them, QI-WOF exhibits a relatively smooth and gradual growth trend across the entire range, and its SWAP and CNOT counts remain at comparatively lower levels than most other algorithms in both compilation frameworks. In contrast, HQAA and GA4QCO show more

noticeable fluctuations and higher metric values in several intervals, while 2QAN follows a similar but slightly higher trend compared to QI-WOF in most cases. These results indicate that QI-WOF maintains a stable variation pattern and relatively lower overhead as the number of qubits increases, and this behavior is consistent under both t|ket⟩ and Qiskit environments.

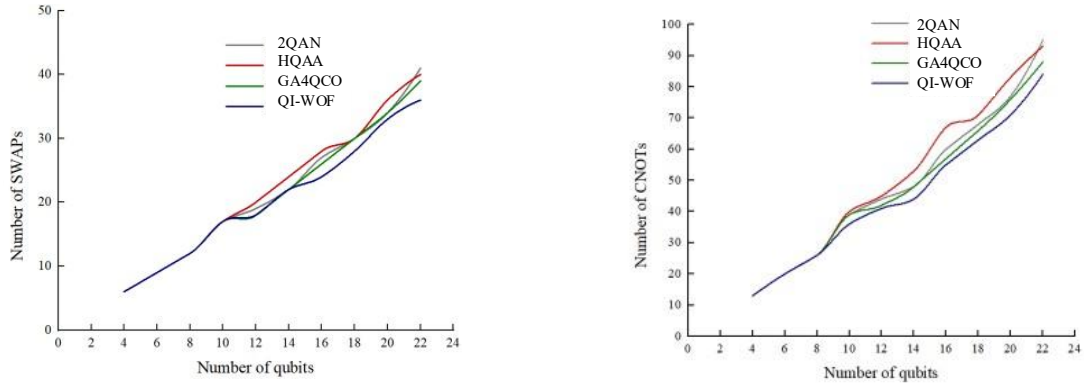

(a) (b)

Figure 7 Trend comparison of metric overhead across different algorithms in t|ket⟩: (a) number of SWAP operations; (b) number of CNOT operations.

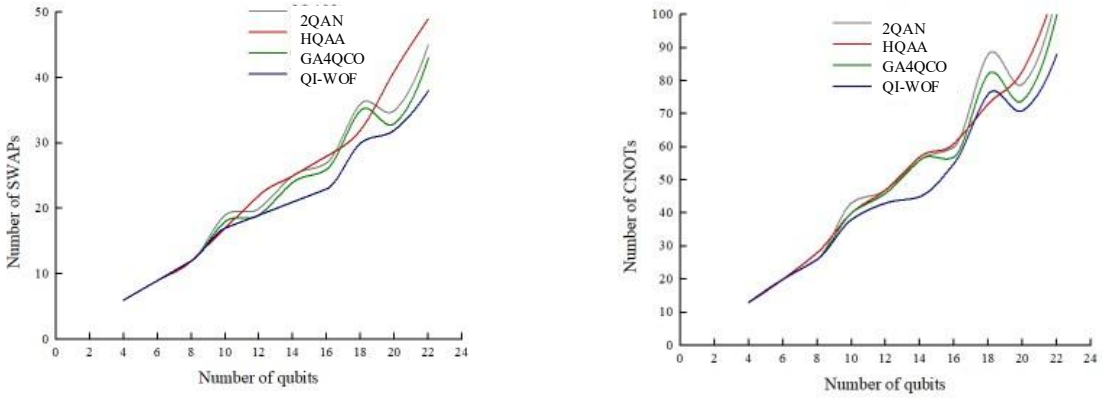

(a) (b)

Figure 8 Trend comparison of metric overhead across different algorithms in Qiskit: (a) number of SWAP operations; (b) number of CNOT operations.

6 Conclusion

This paper presented a quantum-inspired whale optimization framework (QI-WOF) framework for quantum circuit mapping optimization under hardware constraints, which integrates quantum state representation, quantum interference mechanisms, and differential evolution strategies to enhance search diversity and convergence performance. By employing a triple cooperative optimization framework and a nonlinear adaptive regulation mechanism, the proposed method effectively balances global exploration and local exploitation in high-dimensional solution spaces. Experimental results demonstrate that QI-WOF achieves superior convergence accuracy and robustness in classical optimization tasks, while significantly reducing SWAP and CNOT gate overhead in quantum circuit mapping compared with both heuristic methods and population-based algorithms. Moreover, consistent improvements observed across different benchmark circuits and industrial quantum compilers validate its scalability and generalization capability. Overall, QI-WOF provides an efficient and reliable optimization framework for quantum circuit mapping, and it holds strong potential for further extension toward noise-aware optimization and real-world quantum computing applications.

Acknowledgement: The authors acknowledge the support from the School of Computer and Information Engineering, Harbin University of Commerce, Harbin.

Funding Statement: This work was supported by the Natural Science Foundation in Heilongjiang Province of China, under Grant LH2024F042 and by the Science Foundation of Harbin Commerce University, under Grant 2023-KYYWF-0983.

Author Contributions: The authors confirm contributions to the paper as follows: Hui Li was responsible for proposing the algorithmic architecture and coordinating the research; Jie Shen implemented the system; Yingsong Ji drafted the paper and analyzed the experimental results; and Jiepeng Wang assisted in the development of the model and algorithm and provided rigorous review of the manuscript. All authors participated in the algorithm design, reviewed the research findings, and approved the final version of the paper.

Availability of Data and Materials: Data will be made available on request.

Ethics Approval: Not applicable.

Conflicts of Interest: The authors declare no conflicts of interest to report regarding the present study.

Conferences

1. Bernhardt C. Quantum computing for everyone[M]. Mit Press, 2019.
2. Holland C M, Lu Y, Cheuk L W. On-demand entanglement of molecules in a reconfigurable optical tweezer array[J]. Science, 2023, 382(6675): 1143-1147.
3. Main D, Drmota P, Nadlinger D P, et al. Distributed quantum computing across an optical network link[J]. Nature, 2025: 1-6.
4. Zahedinejad E, Ghosh J, Sanders B C. High-fidelity single-shot Toffoli gate via quantum control[J]. Physical review letters, 2015, 114(20): 200502.
5. Cai G, Qiu D. Optimal separation in exact query complexities for Simon's problem[J]. Journal of computer and system sciences, 2018, 97: 83-93.
6. Wu Z, Qiu D, Tan J, et al. Quantum and classical query complexities for generalized Simon's problem[J]. Theoretical Computer Science, 2022, 924: 171-186.
7. Niu S, Suau A, Staffelbach G, et al. A hardware-aware heuristic for the qubit mapping problem in the nisq era[J]. IEEE Transactions on Quantum Engineering, 2020, 1: 1-14.
8. Chen S, Cotler J, Huang H Y, et al. The complexity of NISQ[J]. Nature Communications, 2023, 14(1): 6001.
9. Huang H L, Xu X Y, Guo C, et al. Near-term quantum computing techniques: Variational quantum algorithms, error mitigation, circuit compilation, benchmarking and classical simulation[J]. Science China Physics, Mechanics & Astronomy, 2023, 66(5): 250302.
10. Farhi E, Goldstone J, Gutmann S. A quantum approximate optimization algorithm[J]. arXiv preprint arXiv:1411.4028, 2014.
11. Kikuura S, Igata R, Shingu Y, et al. Performance benchmarking of quantum algorithms for hard combinatorial optimization problems: A comparative study of non-FTQC approaches[J]. arXiv preprint arXiv:2410.22810, 2024.
12. Qiu C, Zhu P, Wei L. A Beam Search Framework for Quantum Circuit Mapping[J]. Entropy, 2025, 27(3): 232.[dio: 10.3390/e27030232]
13. Liu X, Zhang D, Zhang T, et al. A new path plan method based on hybrid algorithm of reinforcement learning and particle swarm optimization[J]. Engineering Computations, 2022, 39(3): 993-1019.[dio:10.1108/ec-09-2020-0500]
14. Steinberg M, Bandić M, Szkudlarek S, et al. Lightcone bounds for quantum circuit mapping via uncomplexity[J]. npj Quantum Information, 2024, 10(1): 113.

15. Booth K E C. Constraint programming models for depth-optimal qubit assignment and SWAP-based routing[J]. arXiv preprint arXiv:2306.08629, 2023.

16. Li Y Z, Liu W, Xu G S, et al. Quantum circuit mapping based on discrete particle swarm optimization and deep reinforcement learning[J]. Swarm and Evolutionary Computation, 2025, 95: 101923.

17. Hartmann J G, Janković D, Pasquier R, et al. Nonlinearity of the Fidelity in Open Qudit Systems: Gate and Noise Dependence in High-dimensional Quantum Computing[J]. Quantum, 2025, 9: 1690.

18. Hu J, Wu H, Zhong B, et al. Swarm intelligence-based optimisation algorithms: an overview and future research issues[J]. International Journal of Automation and Control, 2020, 14(5-6): 656-693.

19. Mirjalili S, Lewis A. The whale optimization algorithm[J]. Advances in engineering software, 2016, 95: 51-67.

20. Wang X, Wei P, Li Y. Enhanced secretary bird optimization algorithm with multi-strategy fusion and Cauchy–Gaussian crossover[J]. Scientific Reports, 2025, 15(1): 23163.

21. Puphasuk P, Wetweerapong J. An enhanced differential evolution algorithm with adaptation of switching crossover strategy for continuous optimization[J]. Foundations of computing and decision sciences, 2020, 45(2): 97-124.

22. Zhu P, Zheng S, Wei L, et al. The complexity of quantum circuit mapping with fixed parameters[J]. Quantum Information Processing, 2022, 21(10): 361.

23. Chou Y H, Cheng-Yen H, Tseng R W, et al. Quantum-Inspired Optimization Algorithm for 3D Multi-Objective Base-Station Deployment in Next-Generation 5G/6G Wireless Network[J]. Computers, Materials, & Continua, 2026, 87(2).

24. Itoko T, Malekakhlagh M, Kanazawa N, et al. Three-qubit parity gate via simultaneous cross-resonance drives[J]. Physical Review Applied, 2024, 21(3): 034018.

25. Simakov I A, Mazhorin G S, Moskalenko I N, et al. High-fidelity transmon-coupler-activated CCZ gate on fluxonium qubits[J]. Physical Review Applied, 2024, 21(4): 044035.

26. Jiang H, Deng Y X, Xu M. Qubit mapping based on Tabu search[J]. Journal of Computer Science and Technology, 2024, 39(2): 421-433.

27. Huang W, Yu H, Ren J, et al. GSLDWOA: A Feature Selection Algorithm for Intrusion Detection Systems in IIoT[J]. Computers, Materials, & Continua, 2026, 86(1): 1.

28. Storn R, Price K. Differential evolution–a simple and efficient heuristic for global optimization over continuous spaces[J]. Journal of global optimization, 1997, 11(4): 341-359.

29. ZULEHNER A, PALER A, WILLE R. An efficient meth-odology for mapping quantum circuits to the IBM QX ar-chitectures[J]. IEEE Transactions on Computer- Aided De-sign of Integrated Circuits and Systems, 2018, 38(7): 1226-1236

30. Lao L, Browne D E. 2qan: A quantum compiler for 2-local qubit hamiltonian simulation algorithms[C]//Proceedings of the 49th Annual International Symposium on Computer Architecture. 2022: 351-365.

31. Steinberg M A, Feld S, Almudever C G, et al. Topological-graph dependencies and scaling properties of a heuristic qubit-assignment algorithm[J]. IEEE Transactions on Quantum Engineering, 2022, 3: 1-14.

32. Sünkel L, Martyniuk D, Mattern D, et al. Ga4qco: genetic algorithm for quantum circuit optimization[J]. arXiv preprint arXiv:2302.01303, 2023.

33. Mirjalili S, Mirjalili S M, Lewis A. Grey wolf optimizer[J]. Advances in engineering software, 2014, 69: 46-61.

34. Marini F, Walczak B. Particle swarm optimization (PSO). A tutorial[J]. Chemometrics and intelligent laboratory systems, 2015, 149: 153-165.

35. Faramarzi A, Heidarinejad M, Mirjalili S, et al. MarinePredators Algorithm: A nature-inspired metaheuristic[J].Expert systems with applications, 2020, 152:113377.

36. Karaboga D. Artificial bee colony algorithm[J]. scholarpedia,2010, 5(3): 6915.

37. Wu G, Mallipeddi R, Suganthan P N. Problem definitions and evaluation criteria for the CEC 2017 competition on constrained real-parameter optimization[J]. National University of Defense Technology, Changsha, Hunan, PR China and Kyungpook National University, Daegu, South Korea and Nanyang Technological University, Singapore, Technical Report, 2017, 9: 2017.

38. S. Sivarajah, S. Dilkes, A. Cowtan, W. Simmons, A. Edgington, R. Duncan, t|ket>: a retargetable compiler for NISQ devices, Quantum Sci. Technol. 6 (1)(2020) 014003.

39. Q. Contributors, Qiskit: An Open-Source Framework for Quantum Computing,Zenodo, Geneva, Switzerland, 2023.